

# Widening the gap between measurement and modelling of secondary organic aerosol properties?

N. Good<sup>1,\*</sup>, D. O. Topping<sup>1,2</sup>, J. Duplissy<sup>3,\*\*</sup>, M. Gysel<sup>3</sup>, N. K. Meyer<sup>4,\*\*\*</sup>, A. Metzger<sup>3</sup>, S. F. Turner<sup>1,\*\*\*\*</sup>, U. Baltensperger<sup>3</sup>, Z. Ristovski<sup>4</sup>, E. Weingartner<sup>3</sup>, H. Coe<sup>1</sup>, and G. McFiggans<sup>1</sup>

<sup>1</sup>School of Earth Atmospheric and Environmental Sciences, University of Manchester, Manchester, M13 9PL, UK

<sup>2</sup>National Centre for Atmospheric Sciences, University of Manchester, Manchester, M13 9PL, UK

<sup>3</sup>Laboratory of Atmospheric Chemistry, Paul Scherrer Institut, 5232 Villigen, Switzerland

<sup>4</sup>ILAQH, Queensland University of Technology, P.O. Box 4233, Brisbane QLD, 4001, Australia

\* now at: Laboratoire de Météorologie Physique, Blaise Pascal Univ., 63000, Clermont Ferrand, France

\*\* now at: Department of Physics, Centre Européen de la Recherche Nucléaire, 1211 Geneva, Switzerland

\*\*\* now at: Laboratory for Energy Systems Analysis, Paul Scherrer Institut, 5232 Villigen, Switzerland

\*\*\*\* now at: Experimental Solid State Physics Group, Blakett Laboratory, Imperial College London, SW7 2BW, UK

## 1 Introduction

The supplementary material aims to quantify the uncertainty associated with the measured growth factors ( $GF_{D_0,RH}$ ) and critical supersaturations ( $S_c$ ) in the context of the models and model sensitivities presented in the manuscript for the unseeded experiments. The measurement uncertainty is shown in Fig. 2 of the original manuscript. The uncertainty in the measured growth factor occurs mainly as a result of the finite ability to accurately and precisely control and measure the flow, voltage and relative humidity (RH) applied to the DMAs (Massling et al., 1999) as well as the finite resolution of the DMA's transfer functions (Cubison et al., 2005; Gysel et al., 2009). When operated un-humidified the uncertainty of the growth factor measured by a TDMA is  $\sim \pm 0.02$ . Humidifying the system increases the uncertainty depending on the accuracy and precision of the RH measurement and temperature control of the DMA (Duplissy et al., 2009).  $\kappa$  values were derived from the unseeded SOA humidograms for each individual HTDMA. The full range of  $\kappa$  values derived from each HTDMA was then used to predict the CCN activity thus bounding the ranged of predictions possible from the HTDMA measurements. The uncertainty of the measured  $S_c(D_0)$  presented in the paper is most significantly due to the ability of the operator to set adequate supersaturations in the CCN counter to constrain the critical point. Only when the properties of the sample aerosol remained constant did the precision/repeatability of the CCN counter's supersaturation settings limit the measurements.

The  $\kappa$  values calculated from the CCN counter's data ( $\kappa_{CCN}$ ) measured simultaneously to the growth factor humidograms after approximately 8 hours of photo-oxidation were  $\sim 0.1$ . It was from this period that the ADDEM water activity parameterisation was derived, as described in the main

text. The range of  $\kappa$  values predicted from the uncertainty in the measured  $S_c$  during this period was used to represent the range of supersaturations. The range of  $S_c$  predicted using the  $\kappa$ -model from the uncertainty in the measured values is illustrated in Supplementary Figs. 1-3 (shaded red to blue). The range of  $\kappa$  values calculated from the uncertainty in each HTMDA's measured growth factor at 90%RH ( $\kappa_{HTDMA}$ ) are shown in Figs. 1-3 (shaded red to brown) for each instrument.

## 2 Supplementary Figure 1 - $H_{MAN}$ 's measurement sensitivity to $\kappa$

Supplementary Figure 1 shows the sensitivity to the measurement uncertainty in  $\kappa$  for  $H_{MAN}$  as described in the introduction. The range of  $\kappa$  as a function of RH (yellow symbols) is within the range of uncertainty in  $\kappa_{H_{MAN}}$  at 90% RH. ADDEM predictions including the effect of bulk to surface partitioning (pink symbols) also fall just above the upper limit of the measured  $S_c$  values. The ADDEM predictions assuming the surface tension of water (red symbols) are above the range of  $S_c$  predicted from the HTDMA. The sensitivity of the ADDEM predictions assuming the surface tension of water to varying the molecular weight (red crosses) and the density (red squares) over the realistic range is small compared to any of the fundamental changes in the model. ADDEM incorporating the parameterised proxy for organic aerosol surface tension (green symbols), results in  $S_c$  lower than the range of  $S_c$  predicted from  $\kappa_{H_{MAN}}$ . Again the sensitivity to varying molecular weight (200-500 $\text{gmol}^{-1}$ ) and density (1200-1800 $\text{kgm}^{-3}$ ) (green crosses and squares respectively) is relatively small compared to more fundamental changes in the models. The ADDEM predictions with the proxy surface tension tend towards the measured values with increasing  $D_0$ .

### 3 Supplementary Figure 2 - $H_{\text{QUT}}$ 's measurement sensitivity to $\kappa$

The data from  $H_{\text{QUT}}$  (shown in Figure 2) for the ADDEM partitioning case (pink symbols) gives  $S_c$  at or slightly above the upper limit of the measured  $S_c$ 's uncertainty. ADDEM including organic surface tension proxy (green symbols) gives  $S_c$ s which tend to the measured values at higher  $D_0$ . The difference between The  $\kappa_{\text{HTDMA}}$  and  $\kappa_{\text{CCN}}$  derived  $S_c$  is even larger than for  $H_{\text{MAN}}$ . The  $\kappa_{\text{HTDMA}}$  and ADDEM predictions assuming the surface tension of water significantly over-predict  $S_c$ .

### 4 Supplementary Figure 3 - $H_{\text{PSI}}$ 's measurement sensitivity to $\kappa$ .

For  $H_{\text{PSI}}$  the range of  $S_c$  derived from  $\kappa_{\text{HPSI}}$  as a result of the uncertainty in  $\text{GF}_{\text{D0,RH}}$  lies within the range of  $S_c$  derived from  $\kappa_{\text{CCN}}$  (the dashed black line indicates the lower limit of  $S_c$  derived from  $\kappa_{\text{CCN}}$  which are otherwise obscured by the HTDMA derived values). The ADDEM prediction incorporating partitioning (pink symbols) fall within or just above the upper limit of the measured  $S_c$ 's uncertainty. The ADDEM predictions assuming the surface tension is that water predict  $S_c$  slightly below the measured values. The ADDEM predictions incorporating the surface tension proxy (green symbols) are below the measurements and their uncertainty.

## 5 Conclusions

Based on the uncertainties presented, the model predictions derived from each HTDMA and their consistency with the CCN measurements generally fall into distinct agreement and disagreement depending on the formulation. For  $H_{\text{MAN}}$ ,  $H_{\text{PSI}}$  and  $H_{\text{QUT}}$  the ADDEM predictions incorporating the surface tension proxy are on or around the upper limit of the measured  $S_c$ 's uncertainty. For  $H_{\text{PSI}}$  the  $\kappa$ -model using  $\kappa_{\text{HTDMA}}$  gives good agreement, whilst for  $H_{\text{QUT}}$  and  $H_{\text{MAN}}$  it is over-predicted. There is a trend of  $\kappa$  increasing with RH for each HTDMA, however this is also within the uncertainty of the  $\kappa$  value at 90% RH, even for  $H_{\text{QUT}}$  which shows the largest variability. The ADDEM predictions assuming the surface tension is that of water do not give agreement using the  $a_w$  derived from any of the HTDMAs. ADDEM incorporating the organic surface tension proxy converges on the measured  $S_c$  at larger diameters for  $H_{\text{MAN}}$  and  $H_{\text{QUT}}$ , it under-predicts  $S_c$  for  $H_{\text{PSI}}$ .

## 6 HTDMA designs

The basic principle of a HTDMA's design is as follows: A single aerosol particle electrical mobility is selected by a differential mobility analyser (DMA). The aerosol selected by

the first DMA (DMA1) should be dry, that is in equilibrium at an RH of less than  $\sim 20\%$  RH. The dry mobility selected sample is then humidified to a set RH. The number size distribution of the humidified sample is then measured by a second DMA (DMA2) operated at the same RH as the humidified sample coupled to a condensation particle counter (CPC). The designs of HTDMAs differ in a number of potentially significant respects. The manner in which the aerosol sampled by the first DMA is dried is not always the same. The DMAs can be operated with closed loop or open sheath flows. Closed loop sheaths recirculate the sheath air therefore gas phase equilibrium is similar to the sample's prior to entering the instrument. Open sheaths may draw the air from the same source as the aerosol sample therefore maintaining the same gas phase composition as the sample. However open sheaths may draw their air from a different source potentially altering gas-particle equilibrium. The humidification of the sample after mobility selection can also be achieved by different techniques. Gore-Tex® membranes are used in some instruments. Passing the sample along a Gore-Tex® tube whilst surrounding it with humid air allows water vapour to diffuse across the membrane humidifying the sample. Similarly Nafion® tubes selectively allow water molecule to pass across them to humidify the sample. Once humidified the number size distribution of the sample is measured. The time the sample spends between the humidifier and the second DMA is known as the residence time. It is important sufficient residence time is allowed so that the sample aerosol reaches equilibrium at the new RH. The second DMA can be humidified independently of the sample (a requirement in open sheath systems) or it may allowed to reach equilibrium with the sample aerosol's RH (possible only in closed loop systems). In order to measure the size distribution of the humidified aerosol the second DMA is operated as a differential mobility particle sizer (DMPS) or a scanning mobility particle sizer (SMPS). Temperature control is very important in the second DMA. A constant temperature is required so that the RH can remain constant. The following sub-sections outline the main design features of the HTMDAs used in this study. Further details are provided in Duplissy et al. (2009) where the same 3 HTDMA's performance is analysed in detail. Note that in Duplissy et al. (2009);  $H_{\text{MAN}}$  is HTDMA3,  $H_{\text{PSI}}$  is HTDMA1 and  $H_{\text{QUT}}$  is HTDMA2.

### 6.1 $H_{\text{MAN}}$

The sample aerosol is generally not dried prior to entering DMA1. DMA1's sheath air is dried to less than  $\sim 20\%$ . A diffusion drier was placed in front of DMA1 for some short periods to check the sample was sufficiently dried. Both of the DMAs are operated as closed loops. A Gore-Tex® membrane is used to humidify the sample aerosol. The membrane is  $\sim 30\text{cm}$  long. A counter flow of humidity controlled air is recirculated around the outside of the Gore-Tex® tube to condition the aerosol. The humidified sample then has a resi-

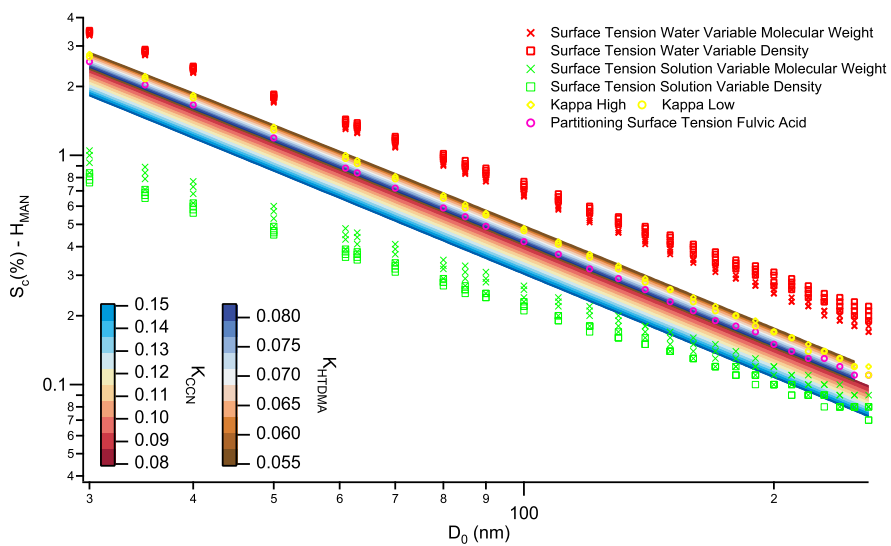


Fig. 1.  $H_{MAN}$ : sensitivity of the  $\kappa$  predictions to the measurement uncertainty.

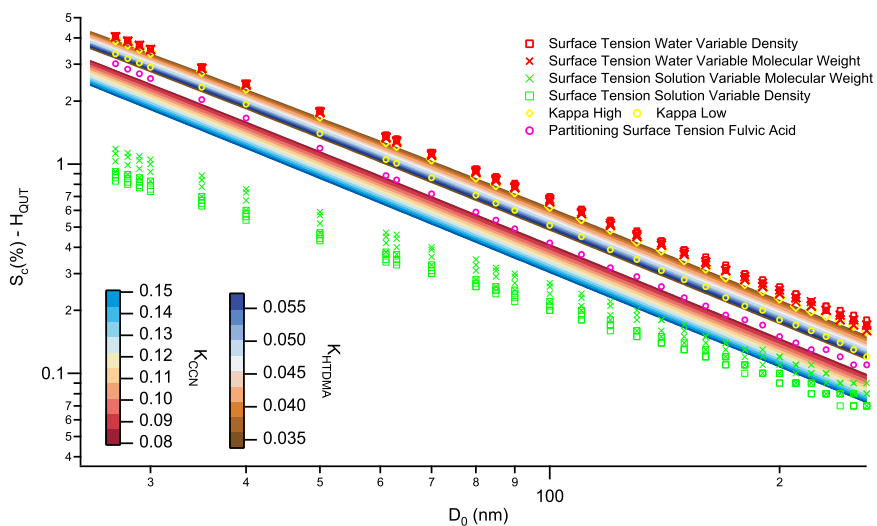
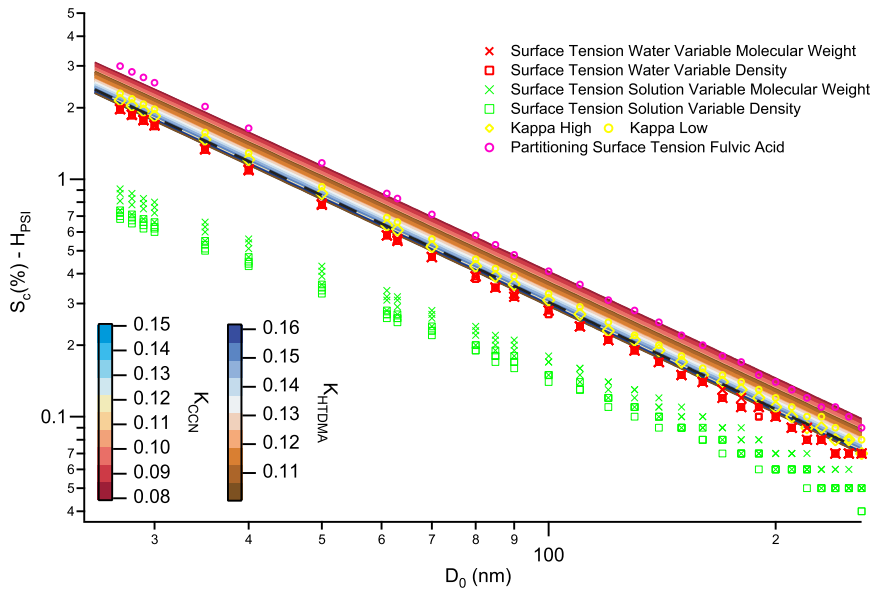


Fig. 2.  $H_{QUT}$ : sensitivity of the  $\kappa$  predictions to the measurement uncertainty.



**Fig. 3.**  $H_{\text{PSI}}$ : sensitivity of the  $\kappa$  predictions to the measurement uncertainty. An additional black dashed line is shown in this figure to indicate the edge of the  $K_{\text{CCN}}$  sensitivity hidden by the  $K_{\text{HTDMA}}$ .

dence time of  $\sim 30$ s before entering DMA2. The temperature across DMA2 was held constant by submersing it in a water bath. The bath was not temperature controlled, but the insulation means that any temperature change occurs slowly such that over a typical measurement cycle ( $< 600$ s) the temperature is constant. The RH obtained in DMA2 is measured using a dew point mirror in the sheath excess, the reference temperature probe is inserted into the DMA itself.

## 6.2 $H_{\text{PSI}}$

The sample aerosol is dried prior to entering DMA1. The DMAs are operated in closed loops. A Gore-Tex® membrane is used to humidify the sample aerosol. DMA1 and the humidifier are located in a temperature controlled box at  $24^\circ\text{C}$ . DMA2 is located in a temperature controlled box at  $20^\circ\text{C}$ . The temperature drop helps the humidification process. The humidified sample has a residence time of 15s (at  $20^\circ\text{C}$ ). A dew point mirror in the sheath excess line is used to determine the RH in DMA2.

## 6.3 $H_{\text{QUT}}$

The sample aerosol is dried prior to entering DMA1. The DMAs are operated in closed loops. A series of Nafion® membranes are used to humidify the sample aerosol and DMA2's sheath air. The residence time of the humidified aerosol prior to entering DMA2 is 4s. The humidifiers and DMA2 are insulated in order to avoid fast temperature changes. A dew point mirror in DMA2's sheath excess is used to determine the RH.

## References

- Cubison, M. J., Coe, H., and Gysel, M.: A modified hygroscopic tandem DMA and a data retrieval method based on optimal estimation, *J. Aerosol Sci.*, 36, 846–865, 2005.
- Duplissy, J., Gysel, M., Sjogren, S., Meyer, N., Good, N., Kammermann, L., Michaud, V., Weigel, R., Martins dos Santos, S., Gruening, C., Villani, P., Laj, P., Sellegri, K., Metzger, A., McFiggans, G. B., Wehrle, G., Richter, R., Dommen, J., Ristovski, Z., Baltensperger, U., and Weingartner, E.: An intercomparison study of six HTDMAs: results and general recommendations for HTDMA operation, *Atmos. Meas. Tech.*, 2, 363–378, 2009.
- Gysel, M., McFiggans, G., and Coe, H.: Inversion of tandem differential mobility analyser (TDMA) measurements, *J. Aerosol Sci.*, 40, 134–151, 2009.
- Massling, A., Wiedensohler, A., and Busch, B.: Concept of an advanced hygroscopic tandem differential mobility analyzer with a great operation stability, *J. Aerosol Sci.*, 30, S395–S396, 1999.